From: Coastal and Estuarine Studies, Vol 42, Nearshore and Estuarine Coh. Sed. Transport, AGU, 1993

A Laboratory Study on the Behavior of Mud from the Western Scheldt under Tidal Conditions

Johan C. Winterwerp, John M. Cornelisse and Cees Kuijper

Preliminary tidal experiments with natural mud from the Western Scheldt in The Netherlands were carried out in an annular flume by varying the flow velocity sinusoidally. After about 10 cycles, a dynamic equilibrium in the suspended sediment concentration was obtained. Prior to slack tide, rapid flocculation was observed in the decelerating phase, resulting in fairly large settling velocities. As a result, a soft bed was deposited with sediment concentrations ranging from about 30 kg/m^3 at the sediment-water interface to about 180 kg/m^3 down within the layer. During the following accelerating phase of the tide, two modes of re-entrainment were observed. Initially, rapid erosion took place, which is attributed to interfacial instabilities. This process is similar to that observed in stratified, two-layer fresh-saline water systems, although the entrainment rate itself appeared to be much smaller. After some time, the intensity of these instabilities decreased, and the soft bed became exposed to smooth surface erosion. This latter process could be described quantitatively with an empirical formula known from literature. It is hypothesized that this two-mode response is caused by a compaction or strengthening of the lower part of the soft bed by cyclic loading due to interfacial instabilities (internal waves).

Introduction

The low lands in The Netherlands are known for their large variety of surface waters. Rivers, channels, lakes, estuaries and coastal waters carry large amounts of fine-grained sediments from the North Sea or from the major rivers. Hence, the beds of several of these waters contain large quantities of mud, and navigation is often hampered by accumulation in the channels. Moreover, many of these sediments are contaminated, giving rise to serious water quality problems. Therefore, Rijkswaterstaat (Ministry of Transport and Public Works, The Netherlands) initiated a long term research program to study the basic processes responsible for the behavior of mud. This program is carried out in close collaboration with Delft Hydraulics and consists, among other studies, of experiments on the erosion and deposition characteristics of natural muds in an

annular flume. These experiments were originally carried out under steady flow conditions. From literature however, it is known that, due to flocculation and bed formation processes, the history of the sediments plays an important role (cf Mehta et al., 1989). This was clearly demonstrated by the results of Umita et al.(1984) showing a significant hysteresis in the sediment concentration during a tidal cycle. Therefore, in addition to the steady state experiments, experiments under dynamic flow conditions were carried out also with sediments from the Western Scheldt in The Netherlands. Results from these experiments are described here.

Sediment Properties

A sediment sample and water were collected in October 1989 in the harbor of Breskens, a small city on the south bank near the mouth of the Western Scheldt estuary in The Netherlands. The sample was taken with a small "Van Veen" grab at a depth of 6.4 m.

Some physico-chemical properties of the sediment are summarized in Table 1, showing that about 1/3 of the sediment consists of clay minerals, with illite as the major fraction. The sample contained a sand fraction of about 1/4. The median settling velocity was measured in the laboratory with a sedimentation balance (flocculated sample) and a sedigraph (dispersed sample) and found to be on the order of 0.1 to 0.2 mm/s. The flow curve of the sediment was measured with two Haake applied-strain roto-viscometers (CV100 and RV100 with measuring elements DA45 and MEII) with a maximum shear rate of 150 s^{-1} obtained in 60 s. The dynamic viscosity, μ, and the Bingham strength, τ_B, are defined from the decelerating curve. They are given in Fig. 1, showing an almost exponential correlation with the sediment concentration, c.

The formation of a bed from a homogeneous suspension with an initial concentration of 60 kg/m^3 was monitored in a small consolidation column of 30 cm height. The development of the sediment-water interface is given in Fig. 2, showing primary consolidation within about 1 day (1440 min). The mean sediment concentration, C_b, within the bed then amounts to about 360 kg/m^3.

The variation of sediment concentration c_b within the bed was measured with an acoustical attenuation probe, the accuracy of which was about 10 %. The concentration profiles show similarity of behavior for different consolidation times, observed earlier by Owen (1975) - see Fig. 3. The depth within the bed z is made dimensionless with the thickness of the bed, H(t), at that moment, and $c_b(z)$ with $C_b(t)$. From Fig. 3 the following correlation was deduced:

$$\frac{c_b}{C_b} = 0.6 \left[\frac{z}{H}\right]^{-0.4} \qquad (1)$$

Table 1. Properties of Western Scheldt Sediment and Pore Water

Mineralogical composition [%]:			
smectite:	3	quartz:	33
chlorite:	7	feldspar:	20
illite:	20	calcite:	12
kaolinite:	<3	dolomite:	3
Sand (>63 μm):	26.6 %	Silt (<63 μm):	73.4 %
Clay (<16 μm):	54.7 %	Lutum (<2 μm):	23.9 %
Organic content:	5.3 %		
Cations:			
Na: 2.8 meq/100g		Ca: 14 meq/100g	
K: 1.3 meq/100g		Fe: 18 g/kg	
Mg: 8.4 meq/100g			
Specific area:	112 m^2/g	CEC: 10	meq/100g
Chlorinity:	17 g/kg	SAR: 36	meq/l
Oxygen content:	5.7 g/m^3	Redox pot:	+170 mV (fluid)
pH:	7.0	Redox pot:	-310 mV (sed.)

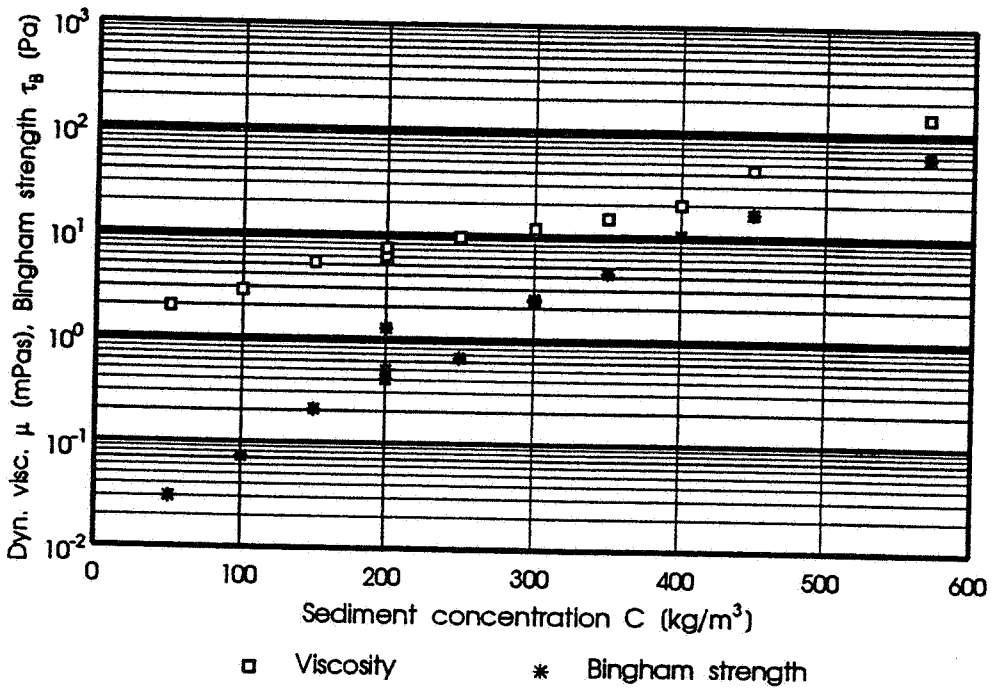

Figure 1. Dynamic viscosity and upper Bingham strength versus concentration.

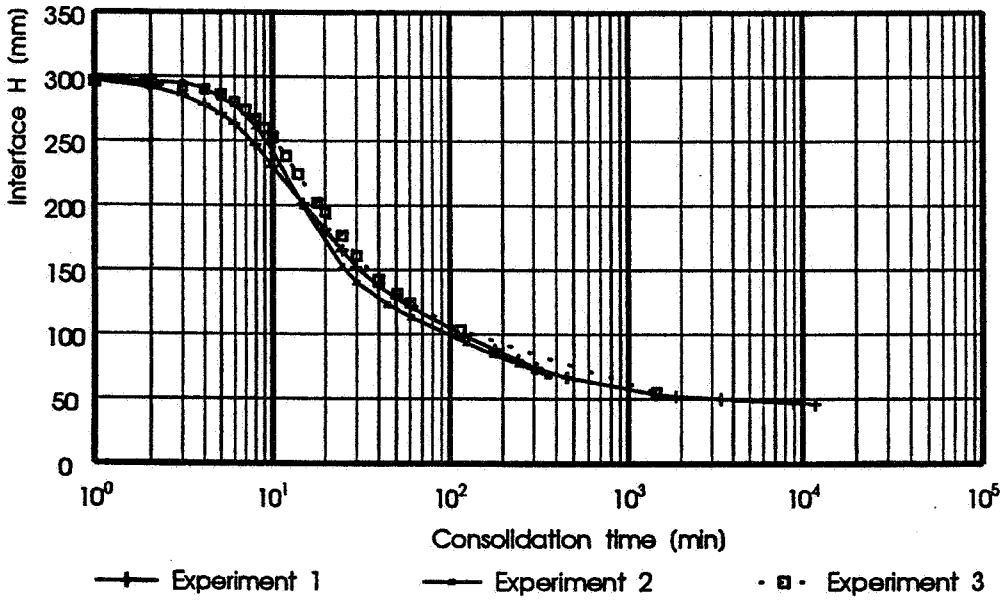

Figure 2. Sediment-water interface during consolidation.

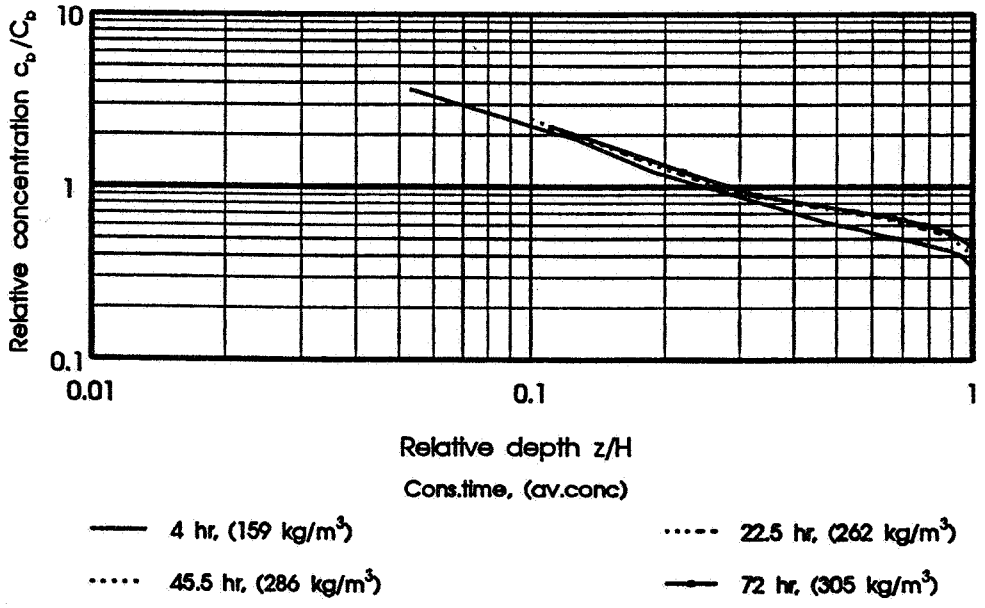

Figure 3. Variation of relative bed concentration during consolidation tests.

where z = 0 corresponds to the bottom of the consolidation column (or the bottom of the annular flume). It was observed that during the bed formation process sorting took place, resulting in low (few %) sand content in the upper part of the bed.

Experimental Facilities and Procedures

The experiments were carried out in an annular flume with a diameter of 2.1 m. Its width is 0.2 m and its depth is 0.3 m. The flow is driven by rotating the upper lid; the effects of secondary currents is minimized by rotating the flume

itself in the opposite direction from the lid. The flume is placed in an isolated room to control temperature, humidity and light access. A detailed description of the facility is given by Kuijper et al. (1989).

During the experiments, the concentration of sediment suspension, c, was measured continuously at mid-depth with an optical sensor. At regular time intervals samples were taken to calibrate this sensor. These samples were also used to measure the variations in grain size distribution during the experiments.

Prior to the experiments, a bed was prepared from the deposition of a homogeneous suspension with an initial concentration of 60 kg/m^3. After a consolidation period of 6 hours, the tidal experiment was started by increasing and then decreasing the flow velocity sinusoidally with a (tidal) period of 12 hours. This was done so that the maximum bed shear stress, τ_b, amounted to 0.4 Pa. After about 10 cycles a dynamic equilibrium was attained and the concentration was measured continuously during another complete cycle. Then the flume was stopped (only upper lid rotation), and photographs and a video recording were made.

Phenomenological Description

The variation of the bed shear stress, τ_b, and sediment concentration, c, during two successive cycles are given as a function of time in Fig. 4 (only 1 out of 5 data points are drawn). Another presentation of the results is given in the c - τ_b graph in Fig. 5. This figure shows that the two semi-cycles are almost identical, indicating a dynamic equilibrium. It also shows a hysteresis between the deposition and the re-entrainment phases, which was observed before by Dyer and Evans (1989) and Costa and Mehta (1990) during measurements in the field.

At about t = 180 min (maximum τ_b) the sediment concentration is slightly above 10 kg/m^3 and remains almost constant till t = 300 min, although τ_b decreases significantly. Around t = 300 min rapid flocculation takes place and flocs on the order of 1 mm are formed, as a result of which rapid deposition occurs. A water-sediment interface is formed similar to that shown in Fig. 2. Initially distinct irrigation channels are observed within the bed, allowing the pore water to escape. These irrigation channels, however, are pressed together around slack tide by self-weight consolidation and/or small stresses induced by the flow. During this deposition process a soft, high concentration layer of about 5 cm thickness is formed. At about t = 400 min rapid erosion occurs. This erosion is attributed to turbulent bursts and breaking of internal waves at the interface (see Fig. 6). This process was described earlier by Srinivas and Mehta (1990). The maximum height of the internal waves was observed to be about 0.5 cm; their wave length about 5 to 8 cm. This picture very closely resembles the entrainment processes observed in stratified flows of fresh and saline waters. The upper few cm of the bed responds to the waves by small, periodic deformations. After 15 to 20 min the amplitude of the waves becomes progressively smaller (see Fig. 7), and the waves vanish at t = 430 min, when

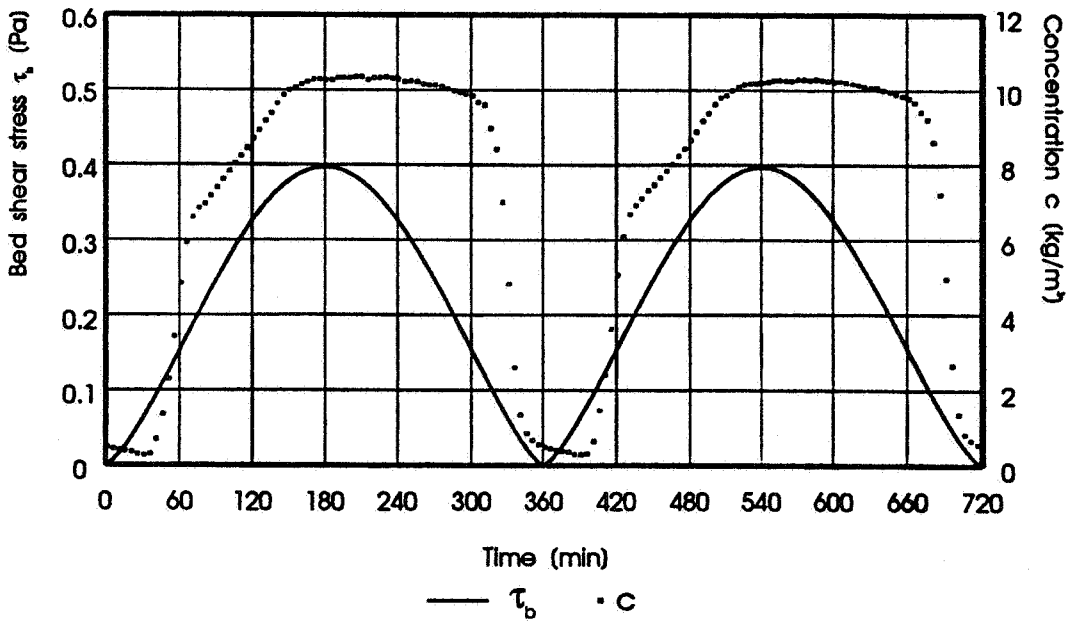

Figure 4. Time variation of bed shear stress and concentration of suspension.

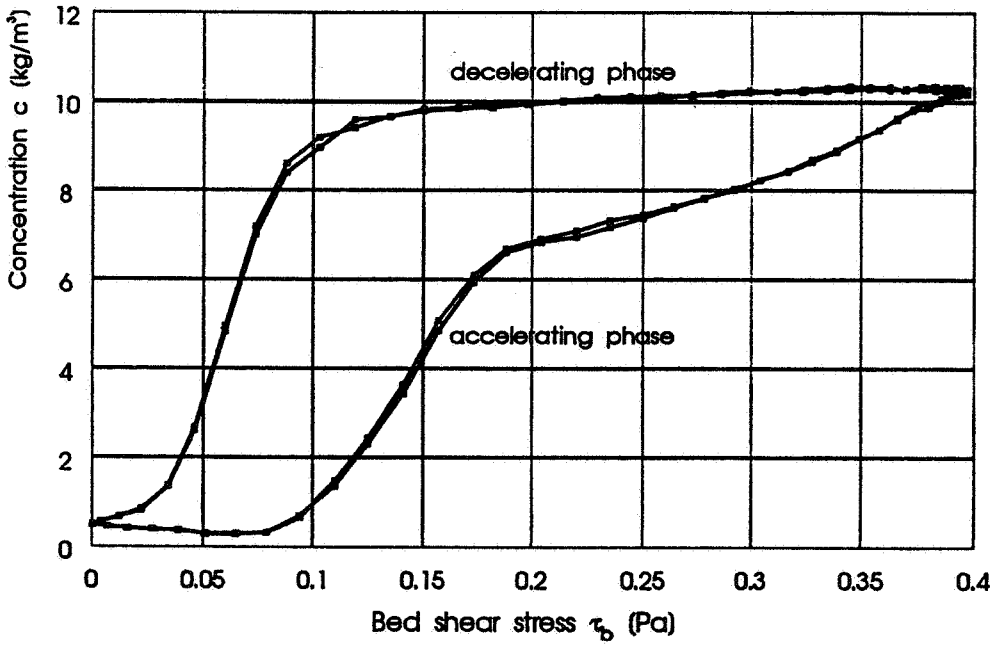

Figure 5. Variation of suspension concentration with bed shear stress.

approximately 3.5 cm of the bed is eroded. The remaining part of the soft bed (thickness about 1.5 cm) is then exposed to smooth surface erosion at a much lower erosion rate, until at t = 540 min τ_b decreases again, and the remaining "non-erodible bed" (thickness of about 3 cm) cannot be scoured anymore. After that, the entire cycle starts again.

A typical feature of this dual-mode response of the bed is the kink in the accelerating c - τ_b curve in Fig. 5. During another series of experiments (not presented here) with $\tau_{b,max}$ = 0.2 Pa, only smooth surface erosion occurred, and no kink was observed in the c - τ_b curve. A close inspection of the results presented by Umita et al. (1984) shows a small tendency of the accelerating

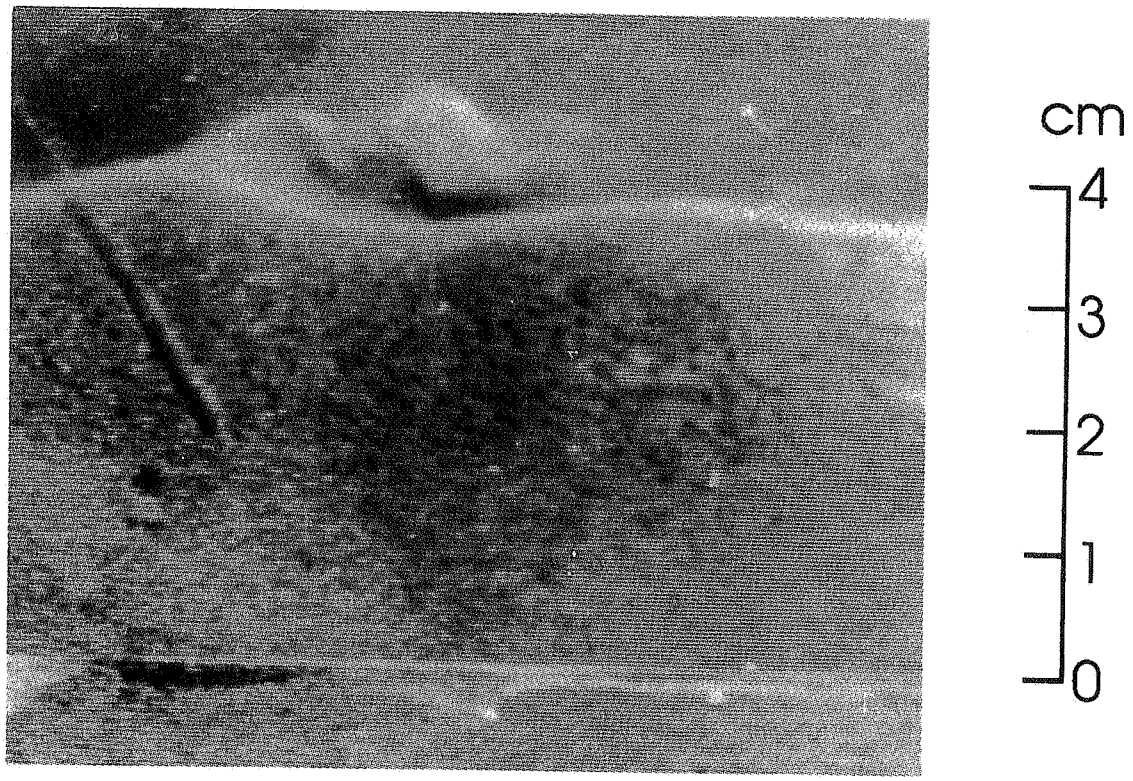

Figure 6. Interfacial instability at t ≈ 420 min.

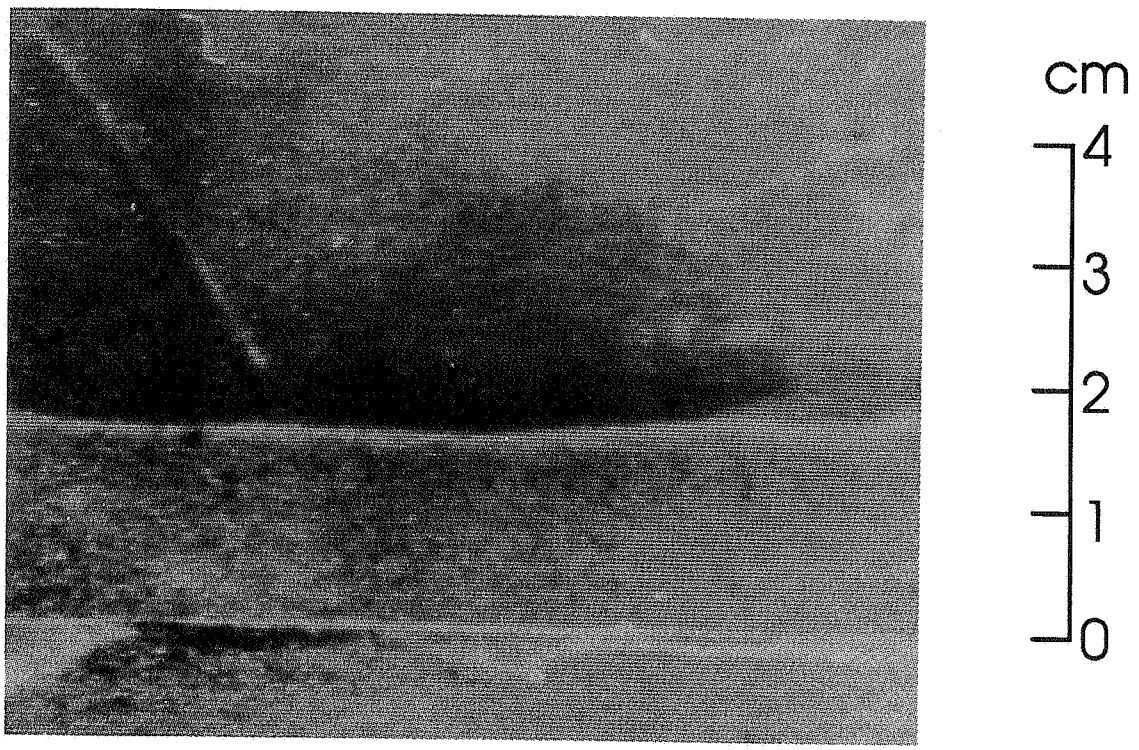

Figure 7. Interface at t ≈ 430 min.

curve to kink, indicating that some entrainment due to internal waves could have occurred, although nothing was mentioned in their paper.

The Depositional Phase

Figure 8 shows a detailed view of the depositional phase from t = 270 till 390 min. The sediment concentration of the suspension c starts to decrease significantly at about t ≈ 315 min, when $\tau_b \approx 0.11$ Pa. The major part of the sediment has deposited at about t = 345 min, $\tau_b \approx 0.03$ Pa. Figure 8 also gives the variation of the deposition rate D, [kg/m^{2}s], defined as:

$$D = h \frac{dc}{dt} \tag{2}$$

where h [m] is the water depth. It is observed that D increases rapidly in about 20 min. Beyond t ≈ 330 min, D decreases again. From D, the settling velocity can be determined. Out of several possibilities the following simple and unambiguous definition is chosen:

$$D = h \frac{dc}{dt} = - W_s c \tag{3}$$

in which W_s [m/s] is an "effective" settling velocity and c the sediment concentration of the suspension. Figure 9 shows W_s as a function of time t. A maximum value of $W_s \approx 0.7$ mm/s is observed around t = 335 min. This value is considerably higher than the median settling velocities of 0.1 to 0.2 mm/s

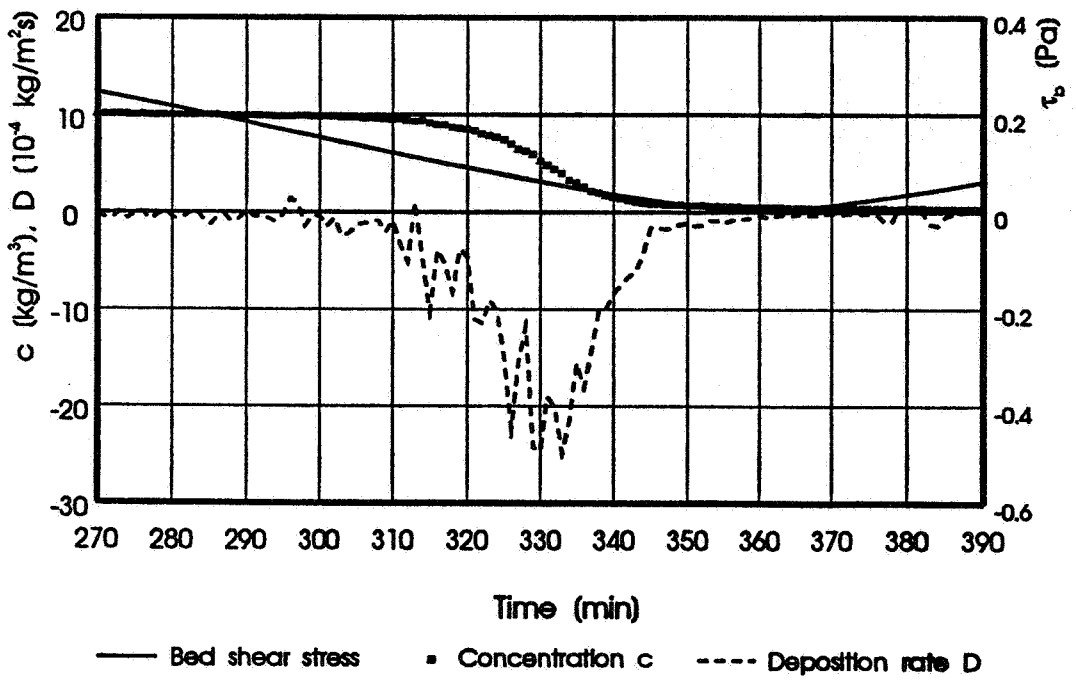

Figure 8. Detailed view of depositional phase (see Fig. 4).

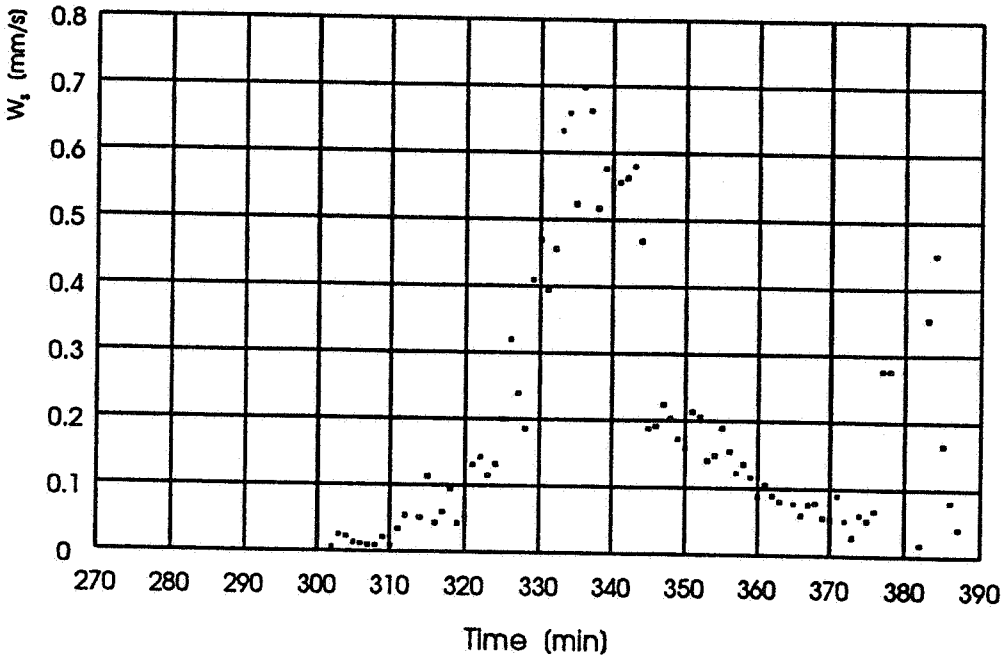

Figure 9. Variation of effective settling velocity with time.

measured with the sedimentation balance and the sedigraph. This is due to the flocculation processes in the high concentrated suspension in the flume, as mentioned earlier.

Flocculation is an aggregation process that occurs when particles adhere to each other due to inter-particle collisions. Hence, the number of particles, i.e. the sediment concentration, is an important parameter in this process. It is therefore common to relate the settling velocity to the sediment concentration. This is done in Fig. 10. In the range of c = 0.4 to 3 kg/m^3 W_s increases by a factor 10. At higher c, W_s first decreases slowly, but near c = 10 kg/m^3, a rapid drop is observed. This drop is related to the definition of W_s: when D $\approx$ 0 (t < 315 min) W_s becomes zero - see the Figs. 8 and 9. The slow decrease in W_s for, say, 5 < c < 8 kg/m^3, can be attributed to the effects of hindered settling. A common description to account for the effects of flocculation and hindered settling is given by Mehta (1986):

$$W_s = k_1 C^n$$
$$W_s = W_{s0} (1 - k_2 C)^{\beta} \qquad (4)$$

Note that the unit of c is kg/m^3. Results for the Severn (Thorn, 1982) and for Tampa Bay (Ross, 1988) are also drawn in Fig. 10, showing that the present data lie well within the same range and show the same trend as those for the Severn and Tampa Bay.

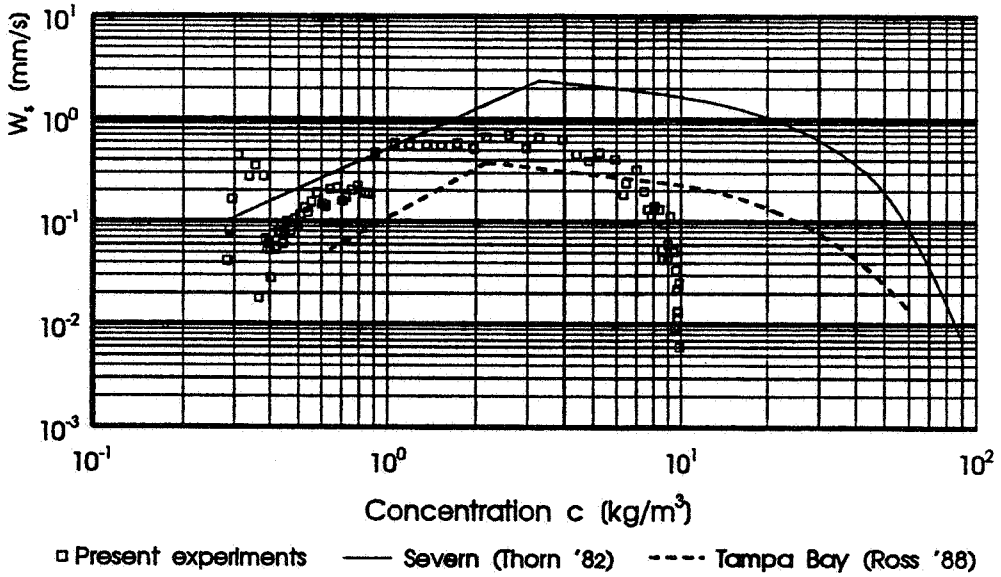

Figure 10. Variation of effective settling velocity with concentration.

The Re-Entrainment Phase

Figure 11 presents a detailed view of the erosion/re-entrainment phase, including the variation in erosion rate E [kg/m^{2}s], which is defined as:

$$E = h \frac{dc}{dt} \tag{5}$$

This figure clearly shows the rapid increase in E up to E = 14×10^{-4} kg/m^{2}s at the beginning of the re-entrainment phase, followed by a rapid drop within 15 to 20 min to about E = 2×10^{-4} kg/m^{2}s. This value is maintained for almost an hour, after which E decreases further to zero.

A quantitative analysis of these results requires information on the sediment concentration within the bed, c_b, and the strength of the bed τ_e (τ_e (z) = critical shear stress for erosion. c_b is determined from Eq. (1), the visually observed thickness of the bed H (from which C_b can be determined), and c. Figure 12 shows the results, yielding the bed concentration distribution $c_b(z)$ at the initiation of re-entrainment (i.e. t $\approx$ 390 min). c_b varies from about 30 kg/m^3 at the water-sediment interface to about 180 kg/m^3 at the bottom of the erodible bed. Within the "non-erodible bed" c_b increases further, its value assessed from the consolidation curve obtained from consolidation experiments.

The strength distribution τ_e [Pa] is estimated using an empirical relationship given by Owen (1975):

$$\tau_e = k_3 \, c_b^{2.3} \tag{6}$$

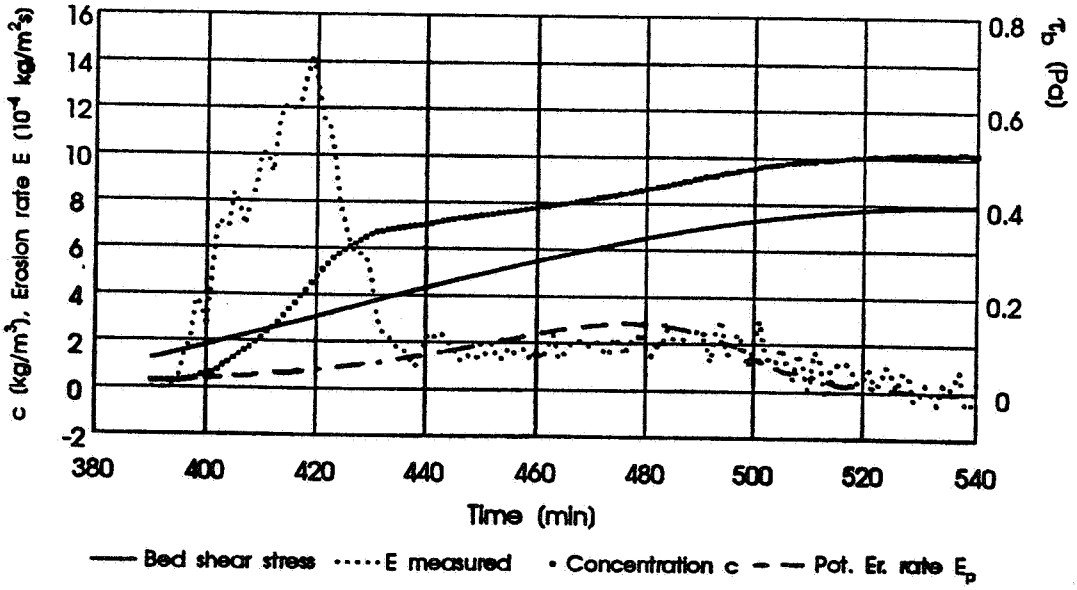

Figure 11. Detailed view erosion phase and potential erosion rate due to Parchure (see Fig. 4).

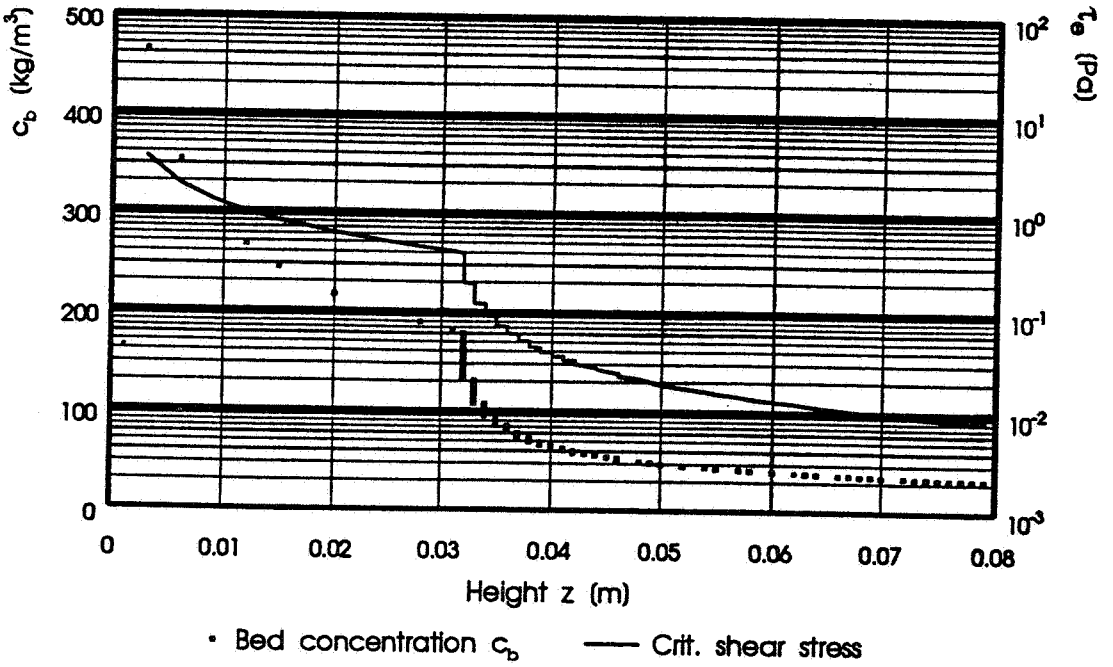

Figure 12. Predicted bed concentration and critical shear stress distribution.

The coefficient k_3 is set at $k_3 = 2.6\ 10^{-6}$, obtained by assuming that $\tau_e = 0.4$ Pa for $c_b = 180$ kg/m^3, i.e. the "non-erodible bed" with a concentration of 180 kg/m^3 at its interface, is not eroded by the maximum current with $\tau_{b,max} = 0.4$ Pa. The resulting $\tau_e(z)$ distribution is also given in Fig. 12, showing a very small strength of about 0.01 Pa at the water-sediment interface. This low value is consistent with the low values of τ_B at low c shown in Fig. 1.

As a first step in the analysis, the erosion formula by Parchure and Mehta (1985) for soft deposited beds is applied:

$$E = E_0 \exp\left[\alpha(\tau_b - \tau_e(z))^\beta\right] \tag{7}$$

in which E_0 is known as the floc erosion rate, τ_b the actual bed shear stress, $\tau_e(z)$ the critical shear stress for erosion, varying with depth, and α and β are parameters. From steady flow experiments in the annular flume with the same mud, α and β could be established: $\alpha = 10\ Pa^{-0.5}$ and $\beta = 0.5$. E_0 is set at $E_0 = 2x10^{-6}\ kg/m^2s$, which is obtained by fitting Eq. (7) with the experimental data ($440 < t < 540$ min). The values of these parameters are in the range of values cited in literature, although E_0 is a little low. By substituting $\tau_e(z)$, as given in Fig. 12, the potential erosion rate E_p can be assessed from Eq. (7). In Fig. 11 E_p and the actual observed erosion rate E are compared. The agreement in the range $440 < t < 540$ min is excellent, indicating that the surface erosion observed in this period can be described with classical formula. Earlier in the re-entrainment phase, the actual erosion rate is underestimated by at least an order of magnitude. This difference can be attributed to different physics prevailing here, i.e. entrainment by the instabilities at the water-sediment interface.

An effort is made to analyze this entrainment process on the basis of classical theory on the stability of stratified fresh-saline water systems. This stability behavior is, in general, related to the gradient Richardson number Ri, defined as:

$$Ri = - \frac{g\left[\frac{d\rho}{dz}\right]}{\rho\left[\frac{du}{dz}\right]^2} \tag{8}$$

Ri can be estimated for the present experiments by substituting for $d\rho/dz$ the mean density difference over the mixed layer with thickness δ_ρ, and for $du/dz = U/\delta_u$, where U is the mean velocity of the flow in the upper layer and δ_u the thickness of the shear layer. From visual observations and velocity measurements with clear water in the flume, the following values for δ could be estimated: $1 < \delta_\rho < 2$ mm, with a mean value $\delta_\rho = 1.5$ mm and $5 < \delta_u < 10$ mm, with a mean value $\delta_u = 7$ mm. This gives the time-variation in Ri of the water-sediment interface as shown in Fig. 13. Because U increases with time, while c_b remains more or less constant, Ri first decreases with time. At the end of the erosional period, U increases only slowly, but c_b starts to grow rapidly, as a result of which Ri increases again. Around $t = 420$ min a kink is observed in the curve - this will be discussed below.

From theoretical analysis a critical value of $Ri = 0.25$ is known, indicating that for $Ri > 0.25$, disturbances cannot grow. From experimental work however, it is known that unstable interfaces may occur for Ri up to 1.

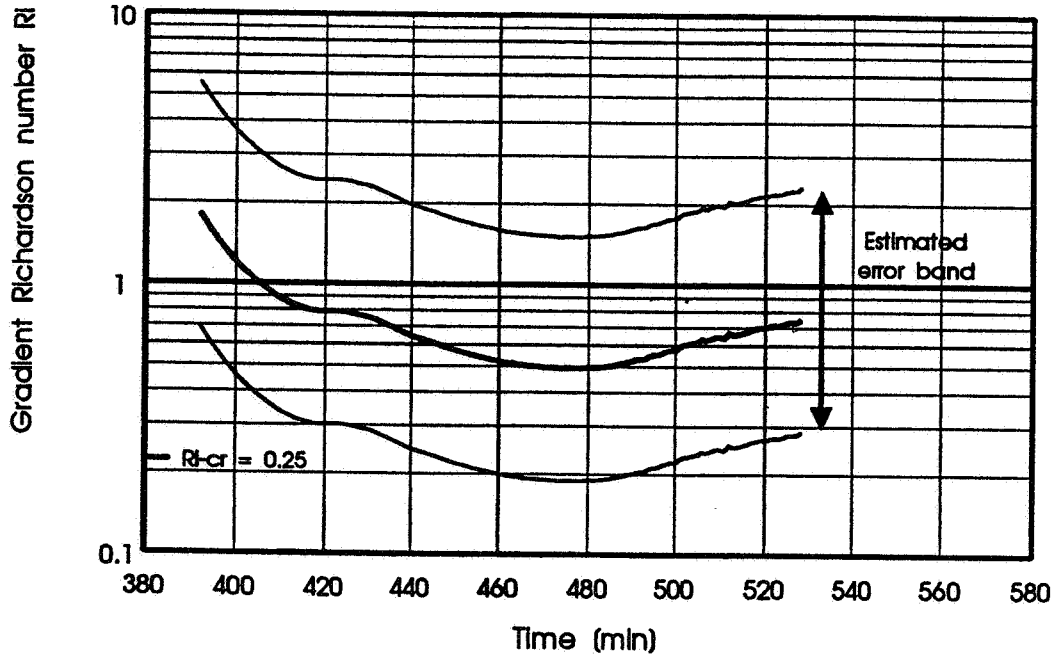

Figure 13. Variation of gradient Richardson number with time.

Figure 13 shows that the estimated Richardson numbers for the present experiments lie well in the range where interfacial instabilities may be expected.

One of the first extensive experimental studies on interfacial instabilities was carried out by Keulegan (1949). His description of the interfacial behavior (cusped, sharp crested waves that break and injection of eddies from the crests into the moving flow) shows a striking resemblance with the present observations and those by Srinivas and Mehta (1990). Another interesting observation, again consistent with the present results, is that the wave length λ was hardly affected by the flow velocity, implying that λ is determined by the stability behavior of the interface. Hence, Keulegan could estimate the minimum possible wave number k_{min} [m] from the wave equation:

$$k_{min} = \frac{2\pi}{\lambda_{max}} = \frac{2\,g}{U_c^2}\,\frac{\Delta\rho}{\rho} \qquad (9)$$

in which U_c is the critical velocity at which the instabilities start to grow (i.e. when entrainment starts). From Fig. 11 it can be seen that $\tau_c \approx 0.07$ Pa, hence $U_c \approx 0.077$ m/s (see Kuijper et al., 1989) for the relation between τ_b and U). Substituting for $\Delta p = 20$ kg/m^3 ($c_b \approx 30$ kg/m^3) and $\rho = 1025$ kg/m^3, $\lambda_{max} \approx 0.10$ m, which is a little larger than the observed wave lengths of 5 to 8 cm.

The gradient Richardson number is difficult to measure during experiments. To analyze experimental data, an overall Richardson number Ri_o is used in general, defined as:

$$Ri_o = \frac{g\ \Delta\rho\ \ell}{\rho\ \chi^2} \tag{10}$$

where ℓ is a typical length scale and χ a typical velocity scale. For appropriate choices of ℓ and χ, Ri_o can be regarded as the ratio between the potential energy required to establish mixing (or the buoyancy effect opposing mixing) and the kinetic energy available for mixing. Various definitions are used in literature. First the approach by Kato and Phillips (1969) and Kantha, Phillips and Azad (1977) is followed, as their experiments with fresh-saline stratified water in an annular flume highly resemble the present experimental set-up. Instead of using the thickness of the mixed layer for ℓ, the water depth h is used:

$$Ri_* = \frac{g\ \Delta\rho\ h}{\rho\ u_{*,s}^2} \tag{11}$$

Here $u_{*,s}$ is the shear velocity [m/s] at the water surface (rotating lid), which can be estimated for roughly the present experiments from a simple equilibrium of forces within the flume, yielding $u_{*,s} \approx 2\ u_*$. The entrainment rate E_* is also related to $u_{*,s}$ and reads:

$$E_* = \frac{u_e}{u_{*,s}} = \frac{E}{c_b\ u_{*,s}} \tag{12}$$

where u_e is the entrainment velocity and E the erosion rate defined in Eq. (5). The variation of E_* with R_i for the present experiments in the period range $390 < t < 440$ min is shown in Fig. 14, together with the results by Kato and Phillips and by Kantha, Phillips and Azad.

Next, a comparison is made with the recent results by Srinivas and Mehta (1990), obtained in a "race-track" flume with kaolinite and bentonite clay. The results are shown in Fig. 15. Ri_o and E_u are defined slightly different:

$$Ri_u = \frac{g\ \Delta\rho\ h}{\rho\ U^2} \tag{13}$$

$$E_u = \frac{u_e}{U} = \frac{E}{c_b\ U} \tag{14}$$

with U = mean flow velocity. Figures 14 and 15 lead to several observations:

1. An inverse trend in the present data is observed around $Ri_* \approx 170$ (and to a lesser extent around $Ri_u \approx 5.5$).

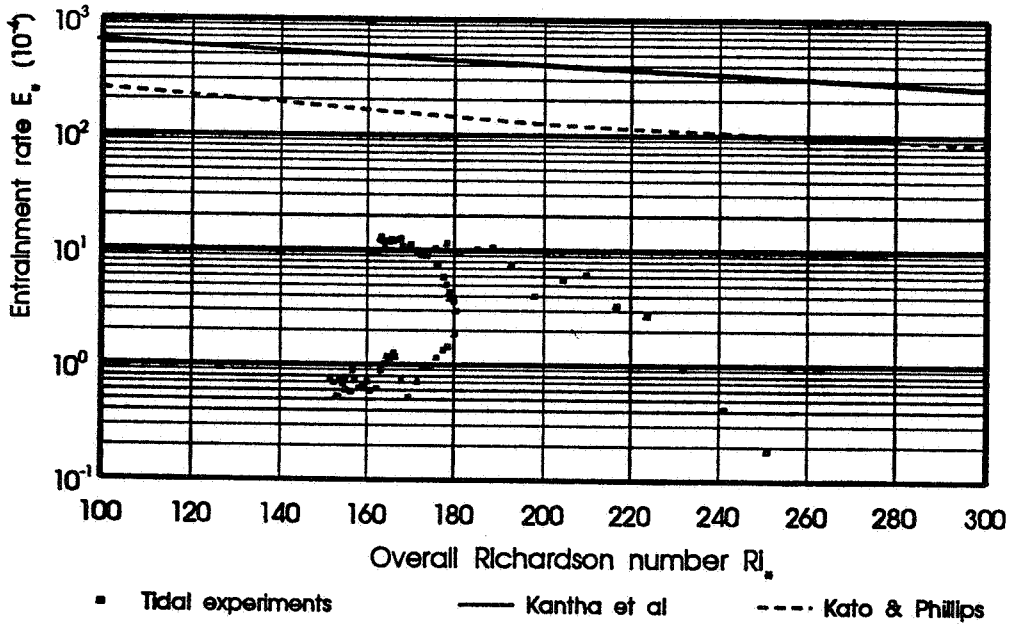

Figure 14. Variation of entrainment rate with overall Richardson number Ri_*.

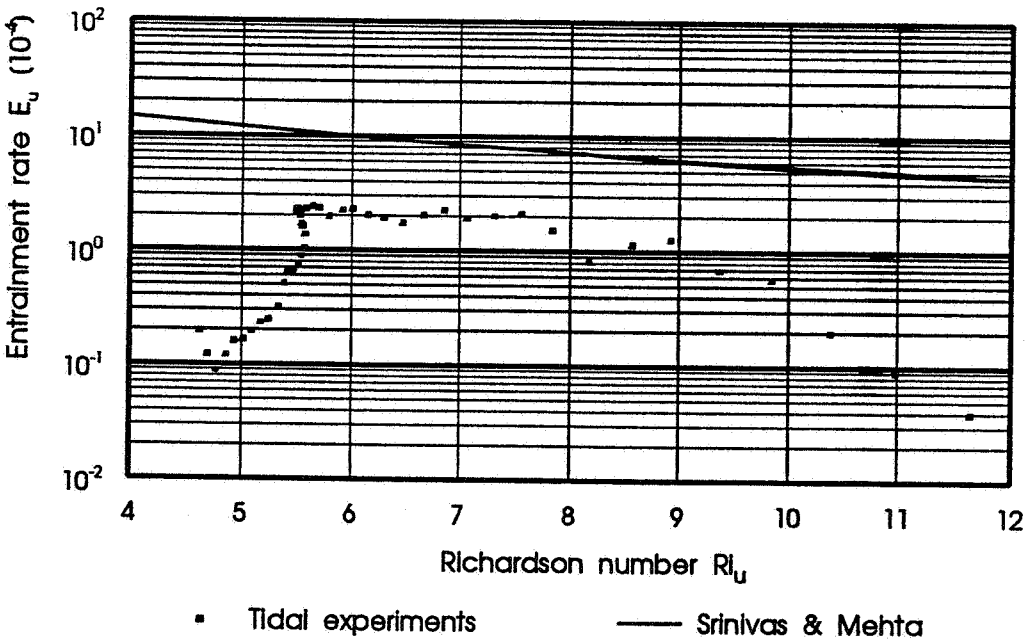

Figure 15. Variation of entrainment rate with overall Richardson number Ri_u.

2. The slope of the data agrees well with the results by Srinivas and Mehta, but only partly with the results by Kantha et al. The present values of E_* and E_u however are (much) smaller.
3. For decreasing Ri, the data show a rapid drop when $Ri_* < 170$, or $Ri_u < 5.5$.

The inverse trend in E_{v*} around $Ri_* = 170$ is due to an inverse trend in Ri_* itself, which is also manifested as a kink in the Ri - t curve around t = 420 min (Fig. 13). This is probably due to a deviation of the c_b profile that is used

(Eq. (1)) from the actual concentration profile; this is elaborated a little further below.

The differences between the present results and those by Kantha et al.and Srinivas and Mehta are significant. Although cohesion (augmented viscosity and yield strength) may play a role, its effect is probably small, as μ and τ_b are small at the concentrations of interest ($c_b \approx 30$ kg/m^3; see Fig. 1), and the experiments by Srinivas and Mehta were also carried out with cohesive material. A second difference between the present experiments and the others is that the present experiments are tidal, i.e. dynamic experiments; thus the interface and the concentration may not respond instantaneously to variations in the bed shear stress. The other experiments are based on equilibrium conditions (steady, uniform flow).

There may be some uncertainties relative to the actual values of the E_* - Ri_* curve around $Ri_* = 170$. However, the results show qualitatively that E_* first increases and then decreases again with increasing Ri_*. Two explanations exist for this behavior, which are at the moment both fairly speculative however, and will be subjected to further research.

From the visual observations and the kink in the c - t curve the soft, high concentrated sediment layer on the bed can be regarded as consisting of two parts. The upper, softer layer behaves as a fluid (viscous part) and is eroded through interfacial instabilities. The lower (elastic) layer is only exposed to surface erosion; no waves can be formed on its interface. During the erosion process, the upper layer becomes thinner, and the waves cannot penetrate as far down into the bed as during the initial phase, and therefore the wave height decreases. As the transfer from one erosion mode to the other is fairly abrupt, some discontinuity in the $c_b(z)$ and/or $\tau_e(z)$ is to be expected. This discontinuity may be formed during the consolidation process around slack tide. This, however is not very likely, as no such behavior was observed during the parallel consolidation experiments. Probably, cyclic loading by the interfacial instabilities themselves may cause additional compaction of the lower layer, causing a discontinuity in the density profile, and thus in the erosion mode. This compaction is not taken into account in Eq. (1). It also explains doubts concerning the inverse trend shown in Fig. 14.

The increase and subsequent decrease in E_* is also possibly due to the character of the interfacial instabilities. At low Ri, i.e. large kinetic energy and/or small buoyancy effects, strong mixing between two layers of fluid may take place. When Ri increases, mixing decreases. This is the classical picture. However, Holmboe (1962) and later for instance Lawrence et al. (1987) observed a second mode of instability when $\delta_u >> \delta_\rho$. Then vortices can develop in the shear layer, not hindered by buoyancy effects. They interfere with the waves at the interface, which become cusped, sharp crested. These waves are known as Holmboe waves, and these are the waves observed in the present experiments, but also by Keulegan (1949), Narimousa et al. (1987), Srinivas and Mehta (1990) and many others. When these waves steepen, they may overtop and inject large quantities of sediment into the flow. It is clear that

in that case, Ri is no longer the sole parameter that describes the stability of the interface. Hence, entrainment may seem to increase with Ri. This picture was quantified by Lawrence et al. (1987) in a stability analysis, showing that the amplification factor is governed by Ri, a wave number, and the ratio δ_u/δ_ρ. For specific combinations of these parameters, the amplification factor may first decrease with Ri, then increase and finally decrease again.

Concluding Remarks

The described experiments have shown that during a tidal cycle a soft high concentrated near-bed sediment layer can be formed, generally referred to in literature as a fluid mud layer. This layer can be exposed to two different modes of erosion/re-entrainment. The first mode, responsible for the erosion of the softer, upper layer is attributed to instabilities of the water-sediment interface. These instabilities closely resemble a pattern known as Holmboe waves. The second mode consists of smooth surface erosion of the lower, more consistent (elastic) layer. This difference in mode must be related to some discontinuity in the bed structure, possibly self-generated by the interfacial instabilities. Detailed measurements near the water-sediment interface and within the bed are necessary to quantify these effects.

Although the present experiments are preliminary and only limited experimental data are available, it can be concluded that care must be taken when applying classical formulas, describing the entrainment processes of two-layered stratified flows to the erosion of fluid mud layers in an estuary.

Acknowledgement

We would like to thank Rijkswaterstaat (Ministry of Transport and Public Works, The Netherlands) for funding this study and for their permission to publish the results. This work is also part of "The Netherlands Integrated Soil Research Program". We would also like to acknowledge the skillful set-up and execution of the experiments by Kees Koree, Frans de Vreede and Erik van Velzen.

References

Costa, R.G. and Mehta, A.J., Flow-fine sediment hysteresis in sediment-stratified coastal waters, *Proceedings of the 22 Coastal Engineering Conference*, Vol 2, 2047-2060, July 1990.

Dyer, K.R. and Evans, E.M., Dynamics of turbidity maximum in a homogeneous tidal channel, *Journal of Coastal Research,* Special Issue No 5, 23-30, 1989.

Holmboe, J., On the behavior of symmetric waves in stratified shear layers, *Geo Fysiske Publikasjoner,* 24, 67-113, 1962.

Kantha, L.H., Phillips, O.M. and Azad, R.S., On turbulent entrainment at a stable density interface, *Journal of Fluid Mechanics,* 79(4), 753-768, 1977.

Kato, H. and Phillips, O.M., On the penetration of a turbulent layer into stratified fluid, *Journal of Fluid Mechanics,* 37(4), 643-655, 1969.

Keulegan, G.H., Interfacial instability and mixing in stratified flows, *Journal of Research of the National Bureau of Standards,* Vol 43, Research Paper RP2040, 487-500, 1949.

Kuijper, C., Cornelisse, J.M. and Winterwerp, J.C., Research on erosive properties of cohesive sediments, *Journal of Geophysical Research,* 94(C10), 14,341-14,350, 1989.

Lawrence, G.A., Lasheras, J.C. and Browand, F.K., Shear instabilities in stratified flow, *Proceedings of the Third International Symposium on Stratified Flows,* February 1987, Pasadena, California, ed. by E.J. List and G.H. Jirka, ASCE, 15-27, 1987.

Mehta, A.J., Characterization of cohesive sediment properties and transport processes in estuaries, in *Lecture Notes on Coastal and Estuarine Studies,* No 14, Proceedings of a Workshop on Cohesive Sediment Dynamics with Special Reference to Physical Processes in Estuaries, ed. by A.J. Mehta, Tampa, Florida, 1984, 290-326, 1986.

Mehta, A.J., Hayter, E.J., Parker, W.R., Krone, R.B. and Teeter, A.M., Cohesive sediment transport. I: Process description, ASCE, *Journal of Hydraulic Engineering,* 115(8), 1076-1093, 1989.

Narimousa, S. and Fernado, H.J.S., On the sheared density interface of an entraining stratified fluid, *Journal of Fluid Mechanics,* 174, 1-22, 1987.

Owen, M.W., Erosion of Avonmouth Mud, Hydraulics Research Station, Wallingford, *Report No INT 150,* 1975.

Parchure, T.M. and Mehta, A.J., Erosion of soft cohesive sediment deposits, ASCE, *Journal of Hydraulic Engineering,* 111(10), 1308-1326, 1985.

Ross, M.A., Vertical structure of estuarine fine sediment suspensions, *PhD Dissertation,* University of Florida, Coastal and Oceanographic Engineering Department, *Report UFL/COEL/TR-079,* 1988.

Srinivas, R. and Mehta, A.J., Observations on estuarine fluid mud entrainment, *International Journal of Sediment Research,* 5(1), 15-22, 1990.

Thorn, M.F.C., Physical processes of siltation in tidal channels, in *Hydraulic Modelling in Maritime Engineering,* Thomas Telford Ltd, London, 1982.

Umita, T., Kusuda, T., Awaya, Y., Onuma, M. and Futawatari, T., The behavior of suspended sediments and muds in an estuary, *Water Science Technology,* 17, 915-927, 1984.